Sirt1 promotes autophagy and inhibits apoptosis to protect cardiomyocytes from hypoxic stress

GUIPING LUO, ZHAO JIAN, YUN ZHU, YU ZHU, BAICHENG CHEN, RUIYAN MA, FUQIN TANG and YINGBIN XIAO

Department of Cardiovascular Surgery, Xinqiao Hospital, Third Military Medical University, Chongqing 400037, P.R. China

Received October 16, 2018; Accepted February 13, 2019

DOI: 10.3892/ijmm.2019.4125

Abstract. Sirtuin 1 (Sirt1) exerts its cardioprotective effects in various cardiovascular diseases via multiple cellular activities. However, the therapeutic implications of Sirt1 in hypoxic cardiomyocytes and the underlying mechanisms remain elusive. The present study investigated whether Sirt1 regulates autophagy and apoptosis in hypoxic H9C2 cardiomyocytes and in an experimental hypoxic mouse model. Right ventricular outflow tract biopsies were obtained from patients with cyanotic or acyanotic congenital heart diseases. Adenovirus Ad-Sirt1 was used to activate Sirt1 and Ad-Sh-Sirt1 was used to inhibit Sirt1 expression in H9C2 cells, in order to investigate the effect of Sirt1 on cellular autophagy and apoptosis. SRT1720, a pharmacological activator of Sirt1 and EX-527, a Sirt1 antagonist, were administered to mice to explore the role of Sirt1 in hypoxic cardiomyocytes *in viv*o. The levels of autophagy and apoptosis-related proteins were evaluated using western blotting. Apoptosis was investigated by TUNEL staining and Annexin V/7-aminoactinomycin D flow cytometry analysis. Heart tissue samples from cyanotic patients exhibited increased autophagy and apoptosis, as well as elevated Sirt1 levels, compared with the noncyanotic control samples. The data from the western blot analysis revealed that Sirt1 promoted autophagic flux and reduced apoptosis in hypoxic H9C2 cells. In addition, Sirt1 activated AMP-activated protein kinase (AMPK), and the AMPK inhibitor Compound C abolished the effect of Sirt1 on autophagy activation. Further exploration of the mechanism revealed that Sirt1 protects hypoxic cardiomyocytes from apoptosis, at least in part, through inositol requiring kinase enzyme 1α (IRE1α). Consistent with the *in vitro* results, treatment with the Sirt1 activator SRT1720 activated AMPK, inhibited IRE1α, enhanced autophagy, and decreased apoptosis in the heart tissues of normoxic mice compared with the hypoxia control group. Opposite changes were observed in hypoxic mice treated with the Sirt1 inhibitor EX-527. These results suggested that Sirt1 promoted autophagy via AMPK activation and reduced hypoxia-induced apoptosis via the IRE1α pathway, to protect cardiomyocytes from hypoxic stress.

Correspondence to: Dr Yingbin Xiao, Department of Cardiovascular Surgery, Xinqiao Hospital, Third Military Medical University, 183 Xinqiao Street, Chongqing 400037, P.R. China
E-mail: xiaoyb@tmmu.edu.cn

Key words: sirtuin 1, autophagy, apoptosis, AMP-activated protein kinase, inositol requiring kinase enzyme 1α, cardiomyocytes

Introduction

Sirtuin 1 (Sirt1), a member of class III histone deacetylases, is a nicotinamide adenine dinucleotide (NAD^+)- dependent histone deacetylase. Recently, it has become clear that Sirt1 deacetylates histone and non-histone proteins to participate in multiple cellular process, including apoptosis, autophagy, calorie restriction, energy metabolism, cell differentiation, anti-aging and DNA damage repair (1-4). Of note, Sirt1 helps cells to cope with environmental stress by targeting abundant transcription factors, such as the Forkhead box O (FOXO) proteins, tumour protein p53, nuclear factor (NF)-κB, peroxisome proliferator-activated receptor-γ coactivator (PGC)-1α, and E2F transcription factor 1 (3,5-7). Previous evidence indicates that Sirt1 exerts a protective role in cardiovascular diseases. Hariharan *et al* (3) have reported that Sirt1 mediates glucose starvation-induced autophagy by deacetylating FOXO in cardiomyocytes. In addition, Sirt1 overexpression protects the heart from ischemia reperfusion injury by inhibiting proapoptotic molecules (8). These studies demonstrate that Sirt1 is involved in cardioprotection.

Hypoxia is the fundamental and inevitable pathophysiological process of cyanotic congenital heart disease (CHD), such as the Tetralogy of Fallot (TOF). Although the underlying mechanism of CHD pathogenesis remains unclear, cardiac apoptotic cell death is vitally important in CHD (9). Of note, previous studies have demonstrated that Sirt1 promoted cellular survival under hypoxic conditions by deacetylating hypoxia-inducible factor (Hif)-1α (10) and Hif-2α (11), implying that Sirt1 may have a critical role in hypoxic environment. Therefore, it is possible that Sirt1 may serve a role in protecting cardiomyocytes from hypoxic injury.

Autophagy is a catabolic process of intracellular degradation in which cytoplasmic materials are recycled through autophagosomal sequestration and subsequent lysosomal degradation (12). Autophagy exists under stress-free conditions to maintain cellular homeostasis. Cardiac-specific deficiency

of the autophagy related 5 (ATG5) gene under physiological conditions induces heart failure in mice, demonstrating that autophagy is required to maintain basal heart function (13). Autophagy has a pivotal role in energy metabolism and protein quality control and has been found to be beneficial to cardiac function in harsh environments, including during ischemia-reperfusion injury (14).

Our group has previously demonstrated that AMP-activated protein kinase (AMPK) protects cardiomyocytes from hypoxia-induced injury through mitophagy (15). In addition, AMPK has been demonstrated to promote autophagy via unc-51 like autophagy activating kinase 1 (ULK1) activation and mammalian target of rapamycin (mTOR) 1 suppression (16). Whether Sirt1 modulates autophagy in hypoxic cardiomyocytes via AMPK has not been fully investigated.

The most conserved endoplasmic reticulum (ER)-resident unfolded protein response (UPR) regulator, the inositol requiring kinase enzyme 1α (IRE1α), functions as a cell fate executor. In response to mild ER stress, the kinase domain of IRE1α is autophosphorylated, subsequently activating its endoribonuclease activity to splice the X-box binding protein 1 (XBP1) mRNA to re-establish protein folding homeostasis. However, under excessive or sustained ER stress, continuous engagement of IRE1α results in events that simultaneously aggravate protein misfolding and apoptosis (17). IRE1α inhibition has been demonstrated to attenuate single prolonged stress-induced neuronal apoptosis in locus coeruleus (18). Furthermore, IRE1α is of vital importance for cytokine-induced apoptosis via c-Jun N-terminal kinase (JNK) activation in human pancreatic beta cells (19,20). Jain *et al* (21) have reported that IRE1α is activated in cardiomyocytes of rats subjected to chronic hypobaric hypoxia, with an accompanying increase in apoptosis. Therefore, it can be hypothesized that Sirt1 may inhibit chronic hypoxia-induced apoptosis through IRE1α.

The present study sought to investigate the role of Sirt1 in modulating autophagy and apoptosis in cardiac cells under chronic hypoxic conditions. The target molecules involved in mediating these effects, such as AMPK and IRE1α, were also assessed.

Materials and methods

Patients studied and myocardial biopsies. A total of 20 patients were enrolled in this study (from January 2015 to January 2017), all of whom underwent surgical correction for congenital heart diseases with extracorporeal circulation in the Department of Cardiovascular Surgery of Xinqiao Hospital (Chongqing, China). Ten patients had cyanotic (4 females and 6 males; mean age, 22 months; 9-32, arterial SpO2, 72%; 63-76) and 10 had acyanotic (4 females and 6 males; mean age, 18 months; 8-27, arterial SpO2, 97%; 95-100) cardiac defects. The relatively normoxic ventricular tissues samples used as control were obtained from patients with ventricular septal defect combined with right ventricular outflow tract obstruction. The hypoxic ventricular tissue samples were obtained from patients with Tetralogy of Fallot (TOF) as previously described (22).

The investigation conformed with the Declaration of Helsinki and was approved by the Human Ethical Committee of Xinqiao Hospital. Informed consent was obtained from all subjects involved in the study prior to surgery.

Adenoviral and lentiviral constructs. The Ad-Easy adenoviral vector system (Qbiogene, Inc., Santa Ana, CA, USA) was used to construct the Ad-Sirt1, Ad-Sh-Sirt1 and Ad-IRE1α, according to the protocol of the manufacturer. A previously reported Sirt1-RNAi sequence was used (23). Ad-LacZ was used as a control. The adenoviruses were transduced at multiplicity of infection (MOI) 50. The Sh-IRE1a and Sh-Scramble lentivirus were purchased from Santa Cruz Biotechnology, Inc. (Dallas, TX, USA). To knockdown IRE1α, H9C2 cells were infected with Sh-IRE1α, and stable cell lines were obtained following puromycin selection.

Cell culture. The H9C2 cell line (American Type Culture Collection, Manassas, VA, USA) was maintained in high glucose Dulbecco's modified Eagle's medium (DMEM; Gibco; Thermo Fisher Scientific, Inc., Waltham, MA, USA), supplemented with 10% fetal bovine serum (FBS; Gibco; Thermo Fisher Scientific, Inc.), 100 U/ml of penicillin, and 100 mg/ml streptomycin at 37˚C. After the indicated treatment, the cells were incubated in serum-free medium overnight. Then, cells in the hypoxia group were placed in a modular incubator (Ruskinn Technology Ltd., Bridgend, UK), containing a gaseous mixture of 94% N_2, 5% CO_2 and 1% O_2 at 37˚C for 24 h. The cells in normoxia group were placed in a 21% O_2 environment. Unless otherwise stated, the hypoxic cells were subjected to hypoxia for 24 h. To inhibit AMPK, Compound C (20 μM; Sigma- Aldrich; Merck KGaA, Darmstadt, Germany) was applied 2 h before hypoxia treatment.

In vivo hypoxia mouse model. Six to eight weeks old C57BL/6J male mice were purchased from the Laboratory Animals Center of Third Military Medical University (Chongqing, China). All animal protocols were performed in accordance with approved principles of laboratory animal care and ethical approval was obtained from the Experimental Animal Committee of The Second Affiliated Hospital of The Third Military Medical University, Chongqing, China.

A total of 40 C57BL/6J mice were randomly divided into four groups: control group, mice placed in a normoxic 21% O_2 environment (21% O_2+DMSO); hypoxic untreated group, mice exposed to hypoxia and treated with vehicle control (10% O_2+DMSO); SRT1720 treated group, mice exposed to hypoxia and treated with SRT1720 (10% O_2+SRT1720); and EX-527 treatment group, mice exposed to hypoxia and treated with EX-527 (10% O_2+EX-527).

O_2 control glove boxes and cabinets (Baker Ruskinn InvivO$_2$ 1000; Ruskinn Technology, Ltd.) were used to maintain a hypoxic environment for the animal studies. The oxygen concentration was stably maintained at 10% O_2 to mimic a hypoxic environment. A carbon dioxide absorbent (Tiger-sorb, Guangzhou, China) was used to remove the CO_2 produced by the mice in the hypoxic chamber.

Drug administration. The Sirt1 specific activator SRT1720 (Selleck Chemicals, Houston, TX, USA) and the Sirt1 inhibitor EX-527 (Sigma-Aldrich; Merck KGaA) were dissolved in dimethyl sulfoxide (DMSO) and diluted to

a final concentration with normal saline to ensure that the final DMSO concentration was 0.5%. To activate or inhibit Sirt1, mice were weighed and injected daily with SRT1720 (50 mg/kg) or EX-527 (10 mg/kg) intraperitoneally for one week prior to hypoxia exposure. The mice in the normoxic or hypoxic control groups received an equivalent volume of diluted DMSO intraperitoneally at the indicated time points. Next, all of the mice in the hypoxic groups were housed in the hypoxic environment (10% O_2) for 2 weeks. During the hypoxia exposure, the mice were administered daily the same drug doses as aforementioned. The normoxic mice were housed in a normoxic environment as a control. The mice were euthanized at the end of the hypoxia experiment and the hearts were harvested for further analysis.

Western blot analysis. Total protein was extracted from the H9C2 cells or heart samples using cell extraction buffer (Invitrogen; Thermo Fisher Scientific, Inc.) supplemented with protease and phosphatase inhibitors (Roche Applied Science, Mannheim, Germany). Protein concentrations from myocardial tissues and H9C2 cells were measured by bicinchoninic acid assay, and then separated (50 μg) by 12% SDS-PAGE gel. Then, protein samples were transferred to polyvinylidene fluoride membranes (Roche Applied Science) and blocked with 5% BSA for 1 h at room temperature. The membranes were probed with the indicated primary antibodies at 4˚C overnight, followed by incubation with horseradish peroxidase (HRP)-conjugated secondary antibodies for 1 h at room temperature, and detection with enhanced chemiluminescence reagents (Beyotime Institute of Biotechnology, Shanghai, China). Changes in protein expression were determined using ImageJ software (National Institutes of Health, Bethesda, MD, USA). The antibodies against microtubule associated protein 1 light chain 3b (LC3B; cat. no. 3868), p62 (cat. no. 39749), phosphorylated (p-) JNK (cat. no. 4668), JNK (cat. no. 9252), p- Jun proto-oncogene (c-jun; cat. no. 3270), c-jun (cat. no. 9165), NF-κB p65 (cat. no. 8242), NF-κB p-p65 (cat. no. 3033), p53 (cat. no. 2524), cleaved Caspase-3 (cat. no. 9661), AMPK (cat. no. 5831), p-AMPK (cat. no. 2535), and β-actin (cat. no. 4970) were used at 1:1,000 dilution and purchased from Cell Signaling Technology, Inc. (Danvers, MA, USA). The antibodies against acetyl-p53 (cat. no. ab61241), IRE1α (cat. no. ab37073), phospho-IRE1α (cat. no. ab48187), Sirt1 (cat. no. ab110304), and Bcl2 (cat. no. ab59348) were used at 1:1,000 dilution and obtained from Abcam. The goat anti-rabbit (cat. no. 7074) and goat anti-mouse (cat. no. 7076) IgG-HRP antibodies were obtained from Cell Signaling Technology, Inc.

Flow cytometry. Cell apoptosis was assessed via an Annexin V-phycoerythrin (PE)/7-aminoactinomycin (AAD) assay. Briefly, after the indicated treatments, H9C2 cells were digested with trypsin, washed twice with cold PBS, collected, and suspended in Annexin V binding buffer. PE-conjugated Annexin V and 7-AAD (BD Biosciences, San Jose, CA, USA) were added to the cells. Following incubation, Annexin V binding buffer was added, and the cell suspensions were analysed by flow cytometry (BD LSRFortessa X-20; BD Biosciences) and data were analysed by Kaluza 2.0 (Beckman Coulter, Inc., Brea, CA, USA).

Determination of apoptosis by TUNEL staining. The apoptosis rates in tissue sections of mouse hearts (prepared as described below for the immunofluorescence experiments) were analysed by TUNEL staining using an *in situ* cell death detection kit (Roche Applied Science), according to manufacturer's protocol. In brief, the slides were incubated with TUNEL reaction mixture solution to mark the apoptotic cells, and the total number of cells was determined using DAPI staining. The slides were visualized under a Leica TCS-SP5 laser-scanning confocal microscope (Leica Microsystems GmbH, Wetzlar, Germany). The apoptotic rate was calculated as a % of the number of TUNEL-positive cells over the total number of DAPI-stained cells.

Immunofluorescence staining. Frozen mouse hearts were embedded in optimal cutting temperature (OCT) compound (Sakura Finetek Inc., Torrance, CA, USA) and 6 μm cryosections were cut. The slides were fixed in 4% paraformaldehyde for 30 min, washed five times with PBS and incubated with 10% goat serum (Boster Biological Technology, Ltd., Wuhan, China) at room temperature. The tissues were immunostained with Hif1α (cat. no. ab1; Abcam; 1:200), α-actin (cat. no. SAB4503474; Sigma-Aldrich; 1:400), cardiac troponin T (TNT; cat. no. ab8295; Abcam; 1:400), or LC3B (cat. no. L7543; Sigma-Aldrich; 1:200), and washed five times with PBS. The samples were then stained with Cy3-labeled goat anti-mouse IgG (cat. no. A0521; 1:500) or Alexa Fluor 488-labeled goat anti-rabbit IgG (cat. no. A0423; 1:500) secondary antibodies (Beyotime Institute of Biotechnology, Shanghai, China) for 1 h at room temperature. The nuclei were counterstained with DAPI. The cells were imaged with confocal laser scanning microscopy (Leica Microsystems GmbH).

Statistical analysis. Data are expressed as the mean ± standard error of the mean. Statistical significance was analysed with GraphPad Prism 5.0 software (GraphPad Software, Inc. La Jolla, CA, USA). Comparisons between two groups were performed by using Student's t-test. Differences among multiple groups were analysed using one-way analysis of variance (ANOVA) followed by Tukey's post hoc test or, two-way ANOVA followed by Bonferroni correction. $P<0.05$ was considered to indicate a statistically significant difference.

Results

Autophagy, apoptosis and Sirt1 are upregulated in cyanotic patients. Specimens of the right ventricular outflow tract were isolated from patients diagnosed with cyanotic or acyanotic congenital heart diseases. Western blot analysis was used to detect the autophagy markers LC3-II and p62, and apoptosis-associated proteins, namely the pro-apoptotic cleaved Caspase-3 and the anti-apoptotic protein Bcl2. The results demonstrated that expression of LC3-II, an indicator of autophagosome accumulation, was increased and while the levels of p62, which is degraded via autophagy, were decreased in the myocardial samples from patients with cyanotic congenital heart disease (Fig. 1A and C). Additionally, the cleaved Caspase-3 levels were increased while the Bcl2 levels were decreased in the cyanotic group (Fig. 1B and C). These

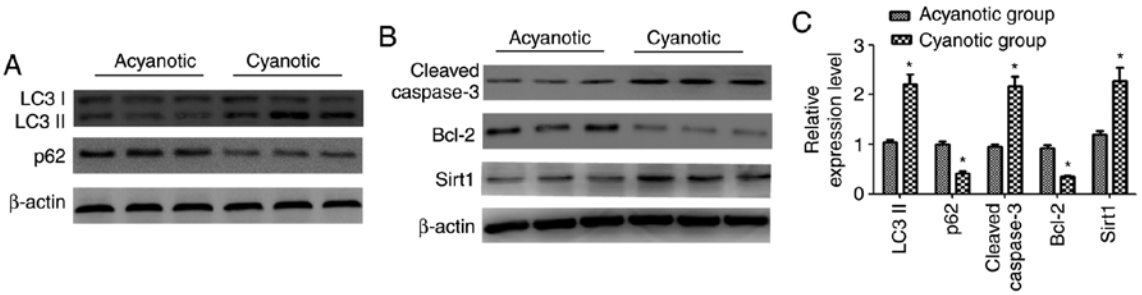

Figure 1. Expression levels of autophagy and apoptosis-related proteins and Sirt1 expression in the myocardium of congenital heart disease patients. (A and B) Representative western blot images of LC3-II, p62, cleaved Caspase-3, Bcl2 and Sirt1 protein expression in myocardial samples from acyanotic and cyanotic patients. (C) Densitometric analysis. n=10, $^{*}P<0.05$ vs. the acyanotic group. Sirt1, sirtuin 1; LC3, microtubule associated protein 1 light chain 3.

results indicated that autophagy and apoptosis were activated in the heart samples of patients with cyanotic congenital heart disease.

Furthermore, to examine whether hypoxia affected cardiac Sirt1 levels, its expression was detected by western blotting. The results revealed that Sirt1 protein expression was increased in the myocardia of cyanotic patients compared with acyanotic controls (Fig. 1B and C).

Sirt1 enhances autophagy in cardiomyocytes. To examine the role of Sirt1 in the autophagy process, Sirt1 was overexpressed in H9C2 cells by use of the Ad-Sirt1 adenovirus, as well as silenced by use of the Ad-Sh-Sirt1 adenovirus. Ad-LacZ was used as control. Fig. 2A illustrates that Ad-Sirt1 successfully increased Sirt1 expression and Ad-Sh-Sirt1 suppressed Sirt1 expression compared with the control group. Ad-Sirt1 stimulated a significant accumulation in baseline levels of LC3-II and a decrease in p62 compared with the control group, indicating that autophagy was activated when Sirt1 was overexpressed (Fig. 2A and B). By contrast, Sirt1 knockdown resulted in p62 accumulation and LC3-II reduction compared with the control group (Fig. 2A and B). To analyse the potential role of Sirt1 in hypoxia-induced autophagy, Ad-Sh-Sirt1-transduced H9C2 cells were subjected to 24 h hypoxia treatment. Knockdown of Sirt1 significantly decreased LC3-II expression and increased p62 expression in hypoxic cardiomyocytes, compared with the hypoxic control group, indicating that autophagy is impaired when Sirt1 is silenced (Fig. 2C and D).

Sirt1 promotes autophagy in hypoxic cardiomyocytes by activating AMPK. To determine whether Sirt1 modulates AMPK in H9C2 cells exposed to hypoxia, the levels of p-AMPK and AMPK were determined. Western blotting revealed that the p-AMPK levels were increased significantly in the Ad-Sirt1 + hypoxia group compared with the hypoxia control group (Fig. 2E and F). Compared with the hypoxia group, the p-AMPK/AMPK ratio was significantly decreased in the Ad-Sh-Sirt1 + hypoxia group (Fig. 2E and F). To investigate whether the pro-autophagy effect of Sirt1 was associated with AMPK, the cells were pretreated with the AMPK inhibitor Compound C (20 μM) along with Ad-Sirt1 prior to the hypoxia treatment. The results demonstrated that the pro-autophagy effect of Sirt1 was reversed when Compound C was added (Fig. 2G and H), suggesting that the ability of Sirt1 to promote autophagy in hypoxic cardiomyocytes is mediated by AMPK.

Sirt1 alleviates hypoxia-induced apoptosis. To determine the effects of Sirt1 on apoptosis in the context of hypoxia, several methods were employed. Western blotting results demonstrated that Sirt1 overexpression attenuated the levels of cleaved Caspase-3 and increased anti-apoptotic Bcl2 expression in hypoxic H9C2 cells (Fig. 3A and B). Furthermore, flow cytometry analysis revealed that the cell apoptosis rate (early apoptotic + late apoptotic) was increased following 24 h induction of hypoxia (Fig. 3C); however, Sirt1 overexpression resulted in a significant decrease in the % of apoptotic cells (Fig. 3C). Collectively, these results revealed that Sirt1 alleviated apoptosis in hypoxic H9C2 cells.

Sirt1 alleviates apoptosis via IRE1α suppression. First, the effects of Sirt1 on the IRE1α pathway were examined by analysing the protein expression levels of IRE1α and its phosphorylated form. As illustrated in Fig. 4A, hypoxia activated IRE1α, as demonstrated by an increase in the p-IRE1α/IRE1α ratio. Ad-Sirt1 transduction significantly reduced the activation of IRE1α, whereas Sirt1 silencing significantly enhanced the activation IRE1α (Fig. 4A and B). These findings demonstrated that Sirt1 regulated hypoxia-induced IRE1α activation.

Next, the role of IRE1α in hypoxia-induced apoptosis in H9C2 cells was investigated. IRE1α was overexpressed in the cells via Ad-IRE1α transduction. To inhibit IRE1α expression in H9C2 cells, stable cell lines were established by transduction with the Lv-Sh-IRE1α lentivirus and subsequent puromycin selection. The protein expression levels of IRE1α were markedly increased or decreased following Ad-IRE1α or Lv-Sh-IRE1α transduction, respectively (Fig. 4C). Western blot analysis was performed to assess changes in the levels of apoptosis-related proteins following IRE1α modulation. After IRE1α overexpression in H9C2 cells exposed to hypoxia for 24 h, the levels of cleaved Caspase-3 were upregulated, while Bcl2 was drastically decreased. However, IRE1α inhibition exerted the opposite effects on the expression levels of these apoptosis-related proteins (Fig. 4C and D).

To explore how IRE1α modulates apoptosis, we investigated whether IRE1α promoted apoptosis by targeting the pro-apoptotic JNK/c-jun pathway in hypoxic H9C2 cells. p-JNK and p-cjun were activated after 24 h hypoxia treatment (Fig. 4C). In addition, the p-JNK/JNK and p-c-jun/c-jun ratios

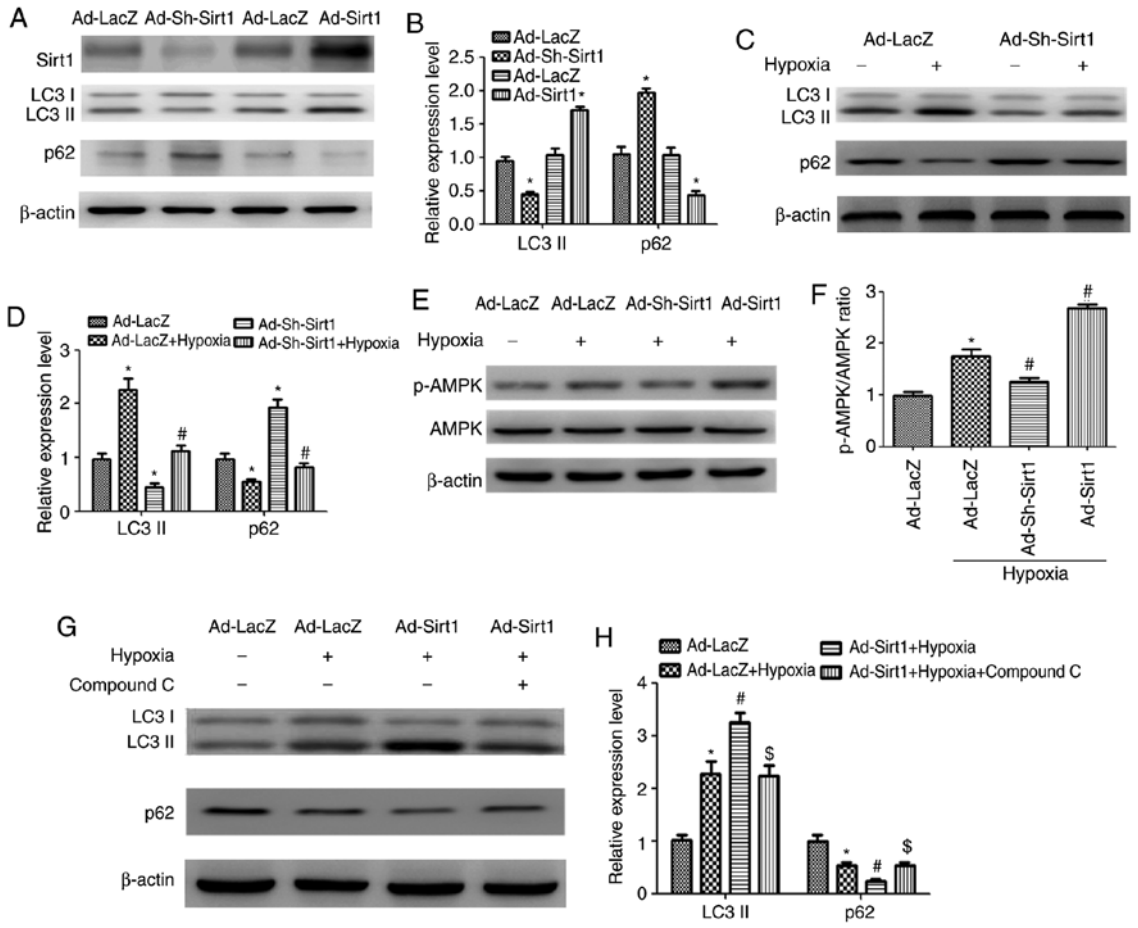

Figure 2. Sirt1 activates AMPK to promote autophagy in hypoxic H9C2 cells. (A) Western blot analysis revealed the expression levels of Sirt1, LC3-II and p62 proteins in H9C2 cells transduced with Ad-Sirt1, Ad-Sh-Sirt1 or Ad-LacZ. (B) The relative protein expression levels as determined by densitometric analysis. (C) Representative blots of LC3-II, p62 and β-actin in H9C2 transduced with Ad-Sh-Sirt1 or Ad-LacZ in the presence of normoxia or hypoxia for 24 h. (D) Densitometric analysis of LC3-II and p62 of H9C2 cells subjected to the indicated treatments. (E) Western blot analysis of AMPK, p-AMPK and β-actin levels after the indicated treatments. (F) Relative levels of p-AMPK vs. total AMPK in each group as determined by blot densitometry. (G) The protein expression levels of LC3-II and p62 in cell lysates were detected by Western blotting after the indicated treatments. (H) Densitometric analysis of the LC3-II and p62 levels in H9C2 cells subjected to the indicated treatments. n=3. *P<0.05 vs. Normoxia + Ad-LacZ group; #P<0.05 vs. Hypoxia + Ad-LacZ group; $P<0.05 vs. Ad-Sirt1 + Hypoxia group. Sirt1, sirtuin 1; LC3, microtubule associated protein 1 light chain 3; AMPK, AMP-activated protein kinase; p-, phosphorylated; sh, short hairpin.

were significantly increased in the Ad-IRE1α+hypoxia group compared with its hypoxia control group (Fig. 4D). Silencing of IRE1α by Lv-Sh-IRE1α decreased the p-JNK/JNK and p-c-jun/c-jun ratios, compared to the Lv-Sh-scramble +hypoxia group (Fig. 4C and D). These results indicated that IRE1α silencing blocked JNK and c-jun activation, leading to decreased cellular apoptosis.

Next, we explored whether IRE1α regulates apoptosis through NF-κB p65. IRE1α overexpression further activated NF-κB p65 in hypoxic H9C2 cells, as demonstrated by a significant increase in the phosphorylation of NF-κB p65 compared with its phosphorylation state in the hypoxic control (Fig. 4C and D). Conversely, IRE1α silencing reversed the regulatory effect of hypoxia on NF-κB p65 activation (Fig. 4C and D). Taken together, these data suggest that IRE1α activation may exert its pro-apoptotic effect through the JNK/c-jun pathway and NF-κB p65.

To determine whether Sirt1 mitigated hypoxia-induced apoptosis through IRE1α, Ad-Sirt1 was coexpressed with Ad-IRE1α. Western blot results demonstrated that Sirt1 and IRE1α coexpression significantly mitigated the IRE1α-dependent increase in apoptosis, as demonstrated by a decrease in cleaved Caspase-3 and an increase in Bcl2 expression compared with the IRE1α + hypoxia group (Fig. 5). In addition, the p-JNK/JNK, p-c-jun/c-jun, and NF-κB p-p65/p65 ratios were decreased in the Ad-Sirt1 + Ad-IRE1α group compared with the ratios in the Ad-IRE1α group (Fig. 5). Taken together, these findings suggest that Sirt1 exerted its anti-apoptotic effects in hypoxic cardiomyocytes by inhibiting IRE1α activation.

Effects of SRT1720 and EX-527 on Sirt1 expression in hypoxic mice. The expression of Hif1α, a marker of hypoxia, was assessed by immunofluorescence staining in control and hypoxic mice. To examine the effects of hypoxia exposure, Hif1α was co-immunolabeled with α-actin, and the nuclei were stained with DAPI, in the heart samples of normoxic and hypoxic mice. The results revealed that the immunofluorescence intensity of Hif1α was markedly increased in the hypoxic group compared with the control mice (Fig. 6A).

To study the functional role of Sirt1 in cardiac protection in hypoxic mice, hypoxia-exposed mice were treated

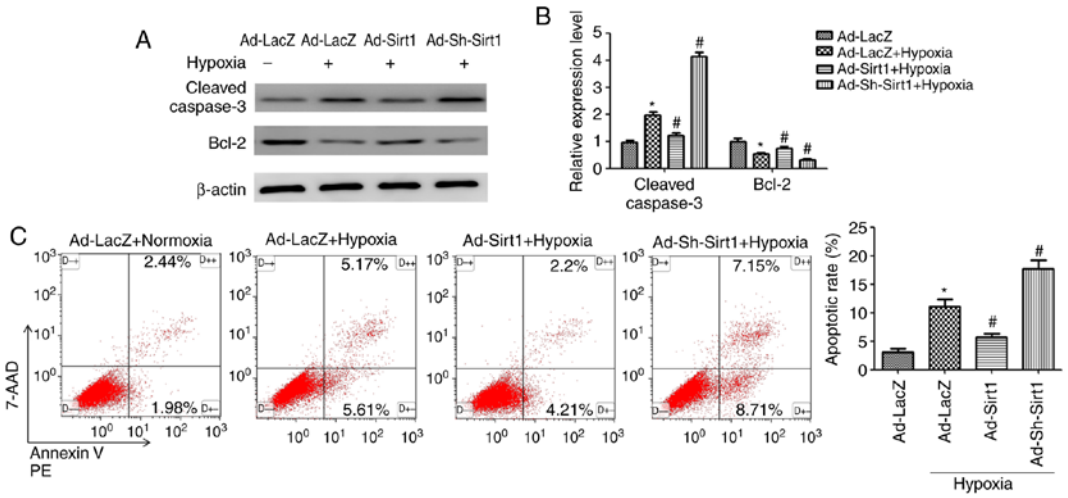

Figure 3. Sirt1 attenuates hypoxia-induced apoptosis in H9C2 cells. (A) Representative western blot images for the expression of apoptosis-related proteins in H9C2 cells subjected to the indicated treatments. (B) Densitometric analysis of the cleaved Caspase3 and Bcl2 levels. (C) Apoptosis was analysed by Annexin V-PE/7-AAD flow cytometry. n=3. *P<0.05 vs. Normoxia + Ad-LacZ group; #P<0.05 vs. Hypoxia + Ad-LacZ group. PE, phycoerythrin; 7-AAD, 7-aminoactinomycin; sh, short hairpin.

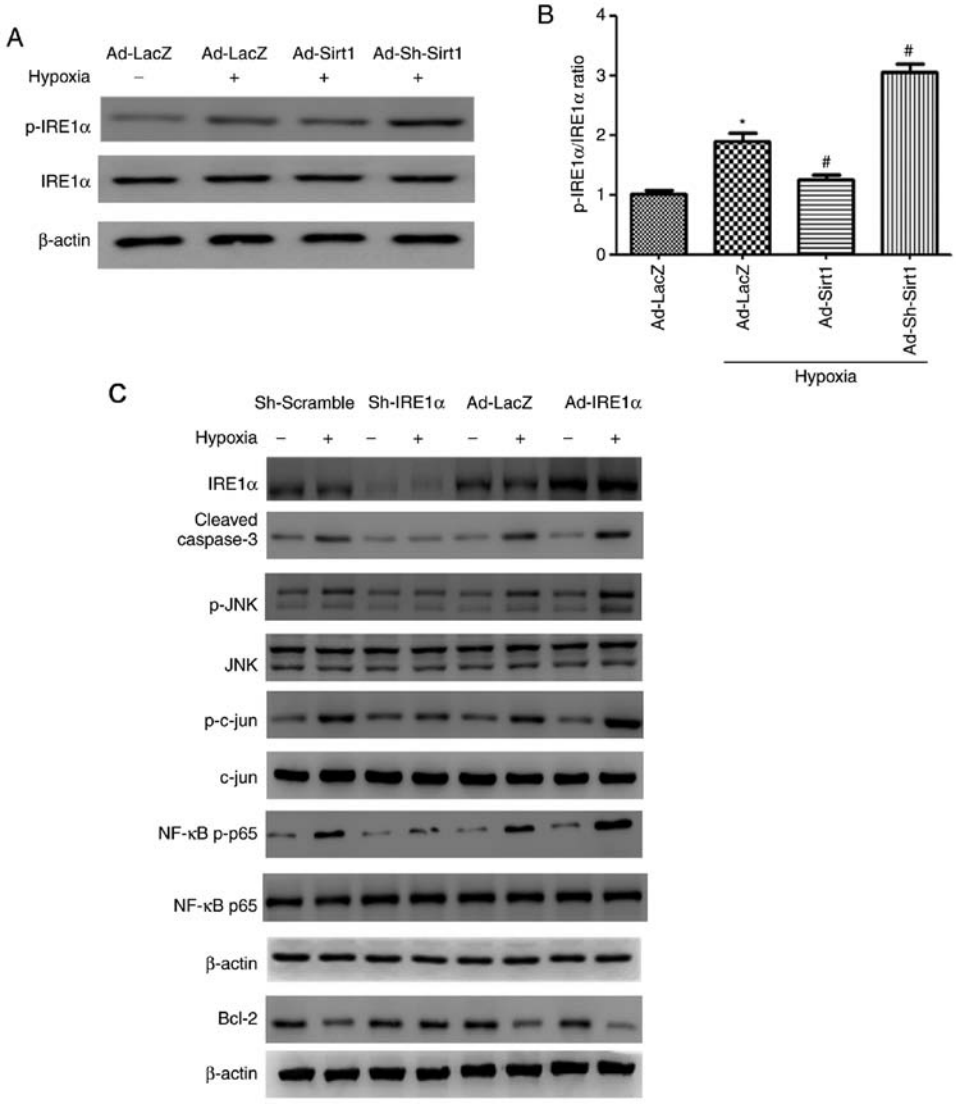

Figure 4. Effect of IRE1α on apoptosis in hypoxic H9C2 myocytes. (A) Western blot analysis of IRE1α, p-IRE1α and β-actin following the indicated treatments. (B) Densitometry analysis of the p-IRE1α/IRE1α ratio levels. n=3. *P<0.05 vs. Normoxia + Ad-LacZ group; #P<0.05 vs. Hypoxia + Ad-LacZ group. (C) Protein levels of IRE1α, cleaved Caspase-3, Bcl2, p-JNK, JNK, p-cjun, cjun, NF-κB p-p65, NF-κB p65, and β-actin in H9C2 cells infected with Ad- IRE1α or Lv-Sh-IRE1α in response to normoxia or hypoxia.

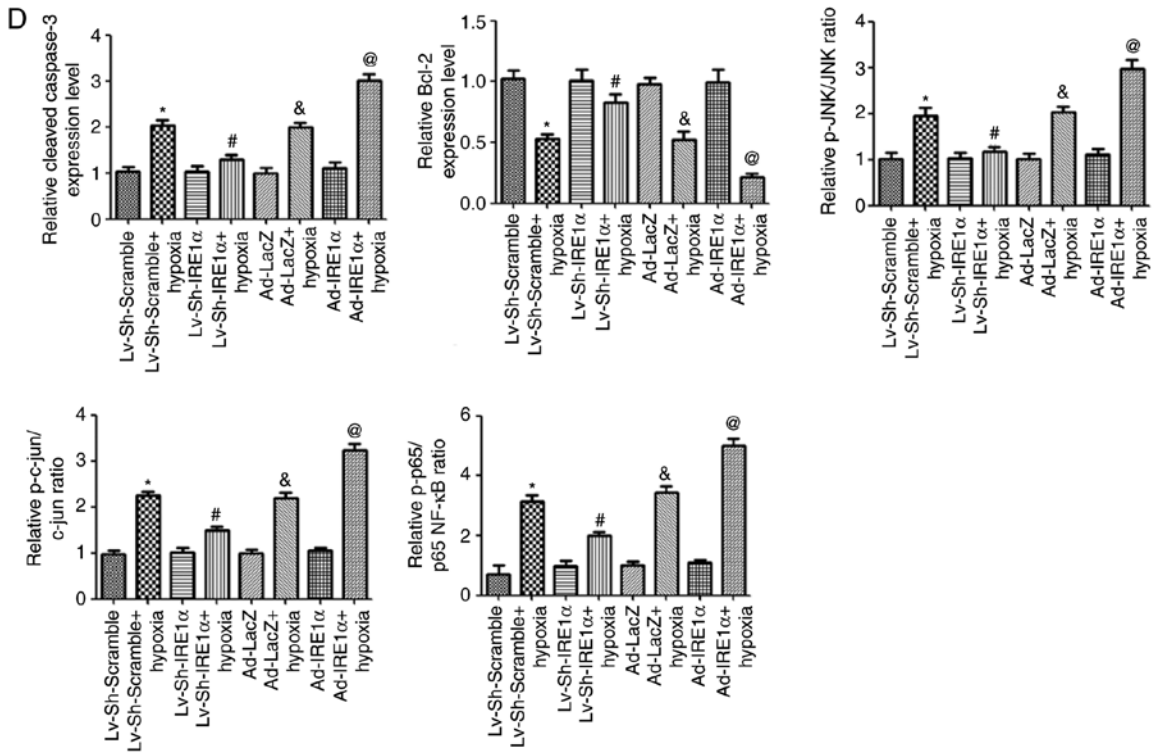

Figure 4. Continued. (D) Densitometric analysis for the western blot data of panel B. n=3. *P<0.05 vs. Lv-Sh-Scramble + Normoxia group; #P<0.05 vs. Lv-Sh-Scramble + Hypoxia group; &P<0.05 vs. Ad-LacZ + normoxia group; @P<0.05 vs. Ad-IRE1α + Hypoxia group. IRE1α, inositol requiring kinase enzyme 1α; p-, phosphorylated; JNK, c-Jun N-terminal kinase; c-jun, Jun proto-oncogene; NF, nuclear factor; sh, short hairpin.

with SRT1720, a Sirt1 activator, or EX-527, a selective Sirt1 inhibitor. As illustrated in Fig. 6B and C, SRT1720 administration increased Sirt1 expression whereas EX-527 treatment suppressed Sirt1 expression in the hearts of hypoxic mice. As p53 is a widely accepted Sirt1 substrate, the acetylation levels of p53 were evaluated in order to determine the deacetylase activity of Sirt1 in the heart samples from the four groups. The acetyl-p53/p53 ratio was increased in the EX-527-treated group, while the ratio was significantly decreased in the SRT1720-treated group, compared with the hypoxia untreated group (Fig. 6B and C). These results demonstrated that SRT1720 and EX-527 administration is effective in modulating the expression and deacetylase activity of Sirt1.

Sirt1 enhances autophagy and inhibits apoptosis in cardiomyocytes of hypoxic mice. To examine whether Sirt1 induced autophagy in the heart, the LC3-II and p62 expression levels were assessed. Long-term treatment with SRT1720 increased cardiac autophagy in hypoxic mice, as indicated by an increase in LC3-II abundance and a decrease in p62 accumulation (Fig. 7A). EX-527 treatment inhibited autophagy in hypoxic mice (Fig. 7A). In addition, AMPK was significantly activated in the heart tissues of mice housed under hypoxic conditions. SRT1720 treatment enhanced the AMPK activation. By contrast, EX-527 administration inhibited AMPK phosphorylation in the myocardium of mice housed in a hypoxic environment compared with the hypoxia untreated group (Fig. 7A).

The immunofluorescence intensity of the LC3B staining in the heart samples was significantly increased in the hypoxic mice, compared with the control group (Fig. 7B). As expected, treatment with SRT1720 induced a significant increase in the LC3B intensity in the hearts from hypoxic mice, whereas EX-527 administration led to a reduced elevation of this marker (Fig. 7B), indicating that Sirt1 increases cardiac autophagic flux *in vivo*.

Next, the expression levels of apoptosis-related proteins were evaluated. Exposure to hypoxia for two weeks resulted in a significant increase in the levels of cleaved Caspase-3, as well as a robust decrease in Bcl2, compared with the control group (Fig. 7C). There was a significant decrease in cleaved Caspase-3 and significant increase in Bcl-2 levels in the hearts of the SRT1720-treated hypoxic mice compared with hypoxic untreated mice. EX-527 treatment resulted in the opposite effects (Fig. 7C). In addition, IRE1α was significantly activated in hypoxic mice, while SRT1720 treatment decreased IRE1α activation. By contrast, EX-527 administration enhanced IRE1α activation in the myocardium of EX-527-treated mice compared with the hypoxia untreated group (Fig. 7C).

Finally, TUNEL staining was used to explore whether Sirt1 activation by SRT1720 in mice could protect cardiomyocytes from hypoxia-induced apoptosis. Hypoxia exposure resulted in a significant increase in the % of TUNEL-positive cardiomyocytes in the wall of the heart (Fig. 7D; P<0.05). Sirt1 overexpression induced by SRT1720 treatment significantly ameliorated the myocardial apoptosis compared the hypoxic untreated mice (Fig. 7D; P<0.05). By contrast, the EX-527-treated hypoxic mice displayed a robust increase in the number of apoptotic cardiomyocytes compared with the hypoxic untreated mice (Fig. 7D; P<0.05). These results indicated that Sirt1 activation in the heart protects cardiomyocytes from hypoxia-induced apoptosis.

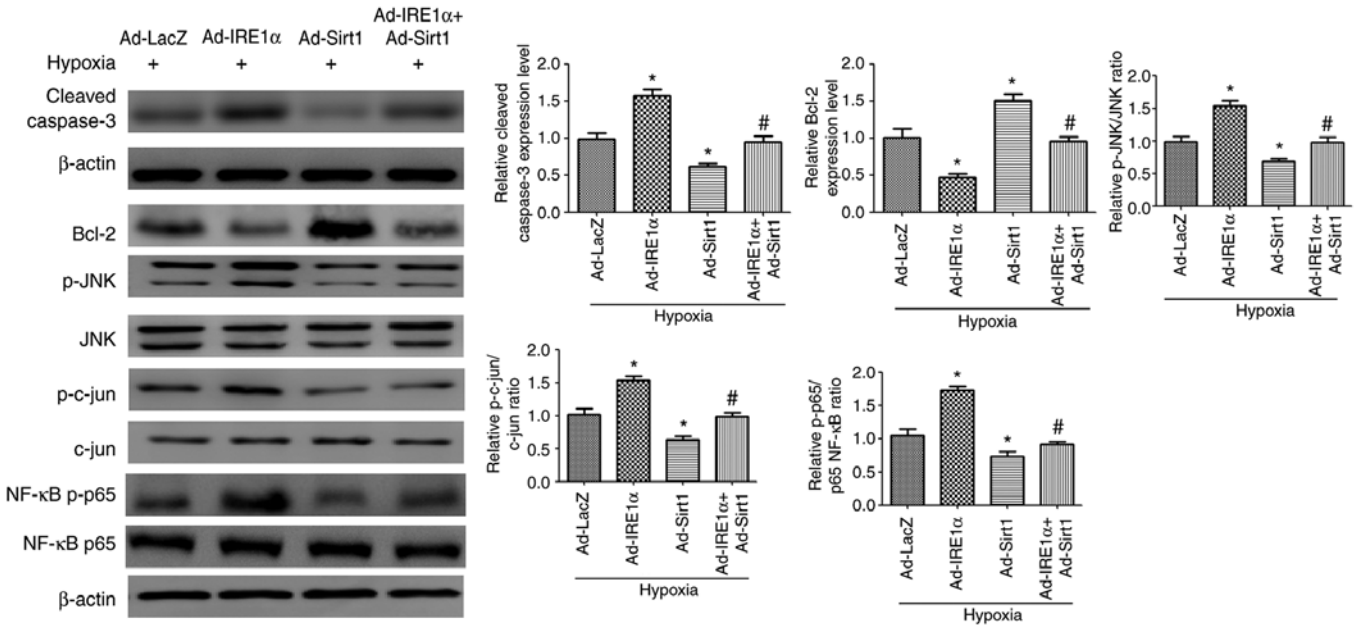

Figure 5. IRE1α promotes apoptosis in hypoxic H9C2 cells, and this effect is reversed by Sirt1 overexpression. Representative blots and densitometry analysis are shown for the protein expression levels of cleaved Caspase-3, Bcl2, p-JNK, JNK, p-cjun, c-jun, NF-κB p-p65 and NF-κB p65, following the indicated treatments. n=3. *P<0.05 vs. Ad-LacZ + Hypoxia group; #P<0.05 vs. Ad-IRE1α + Hypoxia group. IRE1α, inositol requiring kinase enzyme 1α; Sirt1, sirtuin 1; p-, phosphorylated; JNK, c-Jun N-terminal kinase; c-jun, Jun proto-oncogene; NF, nuclear factor.

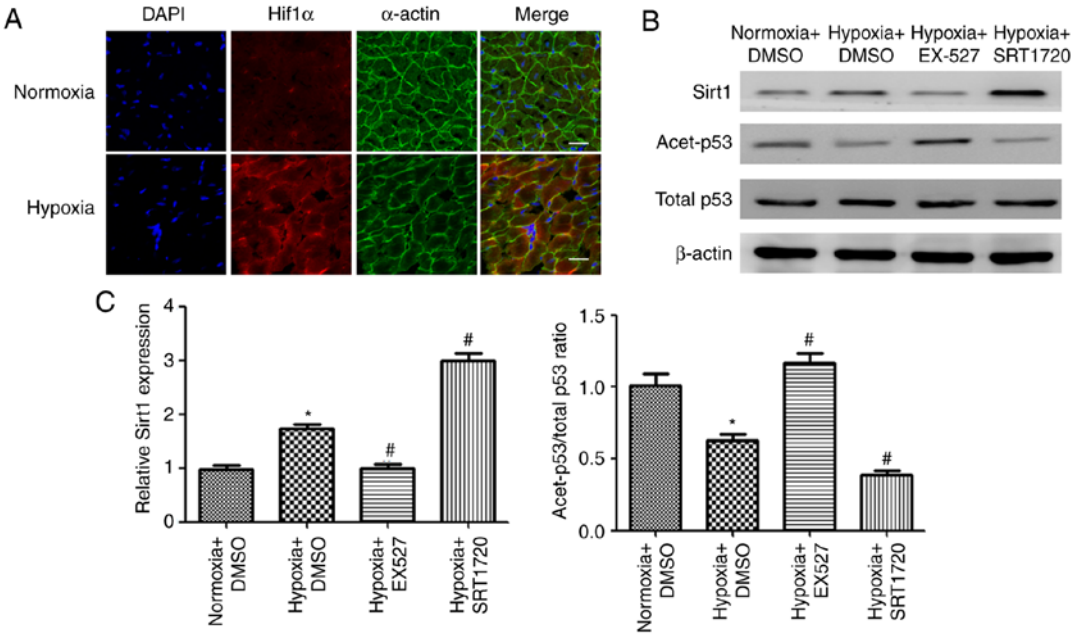

Figure 6. Effects of SRT1720 and EX-527 on cardiac Sirt1 expression in a hypoxic mouse model. (A) Representative confocal images of Hif1α (red), α-cardiac actin (green) and DAPI (blue) in heart samples from normoxic and hypoxic mice (scale bar, 20 μm). (B) Western blot images of Sirt1, acet-p53 and total p53 in heart tissue samples from mice treated as indicated. (C) Densitometric analysis of Sirt1 and ratio of acet-p53/total p53. *P<0.05 vs. Normoxia + DMSO; #P<0.05 vs. Hypoxia + DMSO. Sirt1, sirtuin 1; Hif, hypoxia-inducible factor; acet, acetylated.

These *in vivo* results indicate that Sirt1 enhanced autophagy and protected cardiomyocytes from apoptosis in the heart of hypoxia-exposed mice.

Discussion

Hypoxia is commonly observed in patients with cyanotic congenital heart disease (24), and identifying cellular protective mechanisms that counteract hypoxia-induced injury in cardiomyocytes is of great importance. Tetralogy of Fallot (TOF) is a common cyanotic heart lesion that consists of four anatomical malformations (25). In the present study, it was demonstrated that autophagy and apoptosis are activated in heart samples of cyanotic patients in response to hypoxia. In addition, Sirt1 expression levels were demonstrated to be significantly higher in the samples from the cyanotic group

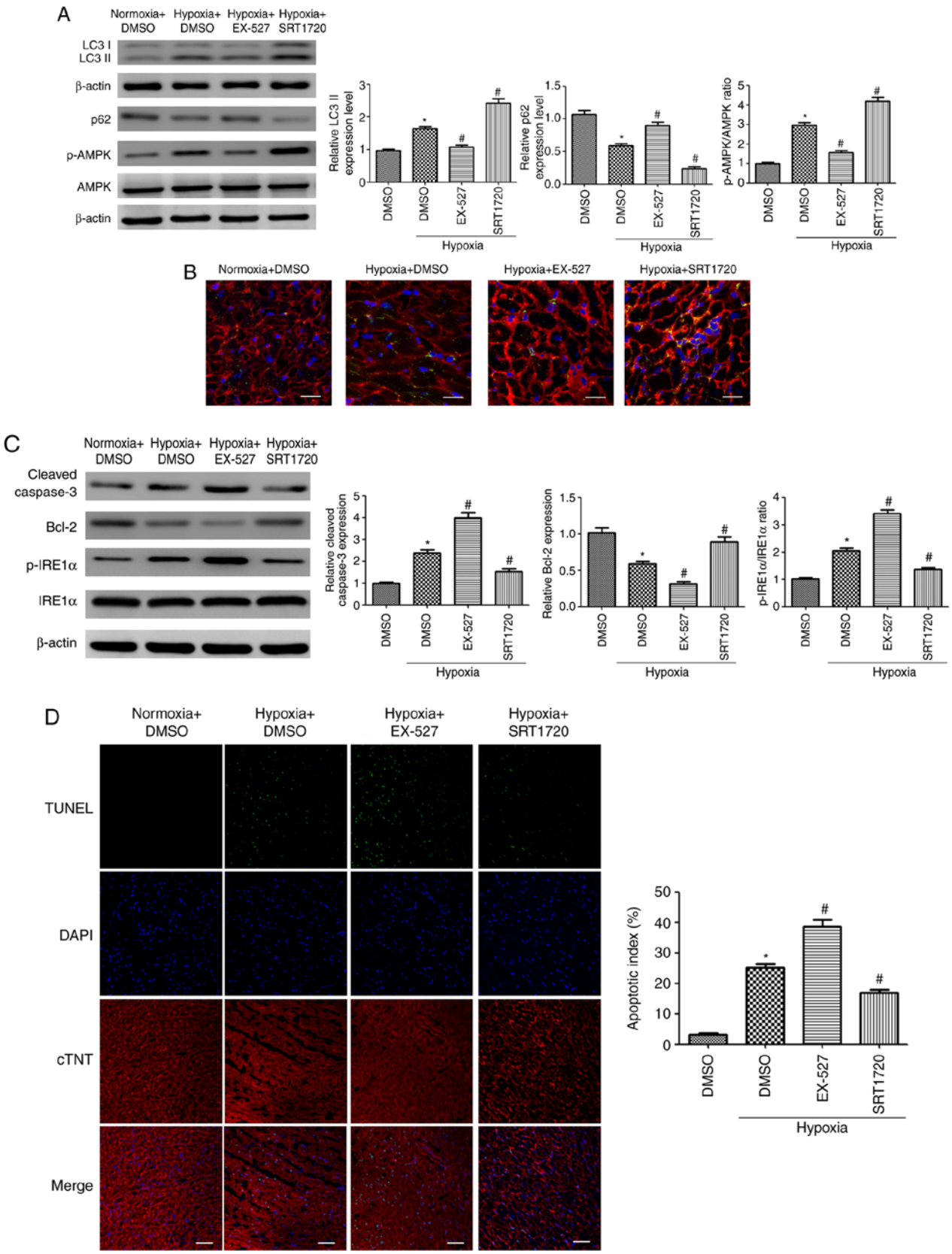

Figure 7. Sirt1 activation enhances autophagy and alleviates apoptosis in the myocardium of hypoxic mice. (A) Representative western blots and densitometric analysis of LC3-II, p62, p-AMPK, AMPK, cleaved Caspase-3 and Bcl2 protein levels in heart samples from mice treated as indicated. (B) Immunofluorescence analysis of LC3B (green) was performed in heart samples from the experimental mice. The cardiomyocytes were costained with c-TNT (red) and the nuclei were stained with DAPI (blue). Scale bar, 20 μm. (C) Representative western blots and densitometric analysis of the p-IRE1α, IRE1α, cleaved Caspase-3 and Bcl2 levels in heart samples of the experimental mice. (D) Representative TUNEL staining images of cardiac tissues from the different groups. The cardiomyocytes were stained with c-TNT (red) and the nuclei were stained with DAPI (blue). The TUNEL staining (green) ratio was counted as the % of apoptotic cardiomyocytes over the total myocytes (Scale bar, 50 μm). n=10. *P<0.05. vs. Normoxia + DMSO group; $^{\#}$P<0.05 vs. Hypoxia + DMSO group. Sirt1, sirtuin 1; LC3, microtubule associated protein 1 light chain 3; p-, phosphorylated; AMPK, AMP-activated protein kinase; c-TNT, cardiac troponin T; IRE1α, inositol requiring kinase enzyme 1α; TUNEL, terminal deoxynucleotidyl-transferase-mediated dUTP nick end labelling.

compared with the samples from the acyanotic controls, indicating that Sirt1 might mediate cellular adaptive response to hypoxia. Owing to the development of ultrasonography used in prenatal diagnosis, the number of patients with congenital heart disease has decreased over the recent years. Therefore, a limitation of the present study is that only ten heart samples were collected for each group. It has been accepted that mammalian cells have developed an adaptive mechanism to activate prosurvival signalling pathways to cope with oxygen level decrease or oxygen deficiency (25,26). Therefore, it can be speculated that upregulation of Sirt1 could be a compensatory mechanism by which cardiomyocytes cope with hypoxic stress.

Accumulating studies have confirmed that Sirt1 has a crucial role in cardiac protection in various cardiovascular diseases through a complex signalling network, including autophagy (3) and apoptosis (23). The present study demonstrated that Sirt1 protected cardiomyocytes from hypoxia-induced apoptosis, at least in part, by inhibiting the IRE1α cascade in cardiomyocytes and by promoting autophagy via AMPK activation. AMPK is a serine/threonine kinase that senses the cellular energy status and regulates energy homeostasis (15). It is widely accepted that AMPK activation inhibits mTOR, leading to enhanced autophagy (16). The present study demonstrated that Sirt1 activated AMPK in cardiomyocytes under hypoxic conditions, and that the pro-autophagy effect of Sirt1 was abolished when AMPK was inhibited. Cells were pre-incubated with Compound C for 2 h prior to hypoxic exposure to inhibit AMPK. In previous studies, the timing of the administration of Compound C before treatments varied from minutes to hours (27-29), suggesting that Compound C has a long term effect in inhibiting AMPK.

Cardiomyocyte apoptosis has a detrimental role in the progression of CHD (9). In the present study, expression of phosphorylated IRE1α was demonstrated to be increased in H9C2 cells exposed to 24 h hypoxia and in heart samples from mice that were exposed to 2 weeks hypoxia. IRE1α overexpression increased the rate of hypoxia-induced apoptosis in H9C2 cells exposed to hypoxia for 24 h, whereas IRE1α inhibition limited apoptosis in H9C2 cells under the same conditions. These results demonstrated that sustained IRE1α activation increases apoptosis in hypoxic cardiomyocytes. It is widely accepted that activated JNK translocates from the cytoplasm to the nucleus, and consequently phosphorylates ser63 and ser73 of transcription factor c-jun, and promotes apoptosis by regulating apoptosis-related proteins (9). NF-κB p65, a member of the NF-κB family, is involved in immune responses and inflammation, and activation of the NF-κB signalling pathway can induce the production of inflammatory cytokines. A recent study revealed that persistent activation of NF-κB was pro-apoptotic in H9C2 cardiomyocytes (30). The current study demonstrated that the IRE1α branch of the UPR promoted apoptosis in chronically hypoxic cardiomyocytes by activating the pro-apoptotic JNK/c-jun signalling pathway and the NF-κB p65 pathway, and that these effects could be reversed by activation of Sirt1. Collectively, the present findings suggest that Sirt1 may exert its protective effects in hypoxic H9C2 cells by decreasing apoptosis via IRE1α inhibition and promoting autophagy through AMPK activation.

To further elucidate the protective role of Sirt1 in hypoxia-induced cardiotoxicity *in vivo*, a hypoxic mouse model was established. SRT1720 and EX-527 were used to modulate the cardiac Sirt1 expression in mice. SRT1720 is a specific and effective Sirt1 agonist, and has been reported to be 1,000-fold more potent than resveratrol (31). EX-527 inhibits Sirt1 by closing the NAD^+ binding site of Sirt1, and it has been widely used as a selective Sirt1 inhibitor (32). Consistent with the *in vitro* results, the *in vivo* study demonstrated that treating hypoxic mice with the Sirt1 agonist SRT1720 limited hypoxia-induced apoptosis and upregulated autophagy in mice housed in hypoxic conditions. EX-527 treatment exhibited the opposite trends. The *in vivo* results support the beneficial pharmacological effect of SRT1720.

Recent studies have revealed that autophagy is closely related to apoptosis (33). Autophagy could block the induction of apoptosis by inhibiting the activation of apoptosis-associated caspases. It is widely accepted that autophagy exhibits a protective role by inhibiting apoptosis (34). Therefore, it is possible that Sirt1 inhibits hypoxia-induced apoptosis in cardiomyocytes partially by promoting autophagy, which needs to be investigated in future studies. The present study has certain limitations. Firstly, only one cell line, H9C2, was used for the *in vitro* experiments. Secondly, further studies will be needed to fully elucidate how Sirt1 regulates AMPK and IREα. The current results, however, suggest that Sirt1 has the potential to favourably modulate autophagy and decrease apoptosis in the context of hypoxic cardiomyopathy, and that the beneficial effects of Sirt1 depend at least partially on AMPK activation and IRE1α inhibition. Therefore, Sirt1 may be a promising protective target to prevent hypoxia-induced cardiac damage.

Acknowledgements

Not applicable.

Funding

This study was supported by the National Natural Science Foundation of China (grant nos. 81770248, 81370004, 81270228 and 81471408).

Availability of data and materials

The datasets used and/or analysed during the present study are available from the corresponding author on reasonable request.

Authors' contributions

GL and YX designed the study. ZJ, BC, and YZ collected and analyzed the data. YZ, RM, and FT edited the language of the manuscript, and were involved in data analysis. All authors have read and approved the final manuscript.

Ethics approval and consent to participate

All protocols involving animals were approved by the Experimental Animal Committee of The Second Affiliated Hospital of The Third Military Medical University, Chongqing, China.

Patient consent for publication

Not applicable.

Competing interests

The authors declare that they have no competing interests.

References

1. Anastasiou D and Krek W: SIRT1: Linking adaptive cellular responses to aging-associated changes in organismal physiology. Physiology (Bethesda) 21: 404-410, 2006.
2. Liu L, Liu C, Zhang Q, Shen J, Zhang H, Shan J, Duan G, Guo D, Chen X, Cheng J, *et al*: SIRT1-mediated transcriptional regulation of SOX2 is important for self-renewal of liver cancer stem cells. Hepatology 64: 814-827, 2016.
3. Hariharan N, Maejima Y, Nakae J, Paik J, Depinho RA and Sadoshima J: Deacetylation of FoxO by Sirt1 plays an essential role in mediating starvation-induced autophagy in cardiac myocytes. Cir Res 107: 1470-1482, 2010.
4. Liu B, Ghosh S, Yang X, Zheng H, Liu X, Wang Z, Jin G, Zheng B, Kennedy BK, Suh Y, *et al*: Resveratrol rescues SIRT1-dependent adult stem cell decline and alleviates progeroid features in laminopathy-based progeria. Cell Metab 16: 738-750, 2012.
5. Yang Y, Duan W, Li Y, Jin Z, Yan J, Yu S and Yi D: Novel role of silent information regulator 1 in myocardial ischemia. Circulation 128: 2232-2240, 2013.
6. Alcendor RR, Gao S, Zhai P, Zablocki D, Holle E, Yu X, Tian B, Wagner T, Vatner SF and Sadoshima J: Sirt1 regulates aging and resistance to oxidative stress in the heart. Circ Res 100: 1512-1521, 2007.
7. Ding C, Zou Q, Wang F, Wu H, Wang W, Li H and Huang B: HGF and BFGF secretion by human adipose-derived stem cells improves ovarian function during natural aging via activation of the SIRT1/FOXO1 signaling pathway. Cell Physiol Biochem 45: 1316-1332, 2018.
8. Hsu CP, Zhai P, Yamamoto T, Maejima Y, Matsushima S, Hariharan N, Shao D, Takagi H, Oka S and Sadoshima J: Silent information regulator 1 protects the heart from ischemia/reperfusion. Circulation 122: 2170-2182, 2010.
9. He S, Liu P, Jian Z, Li J, Zhu Y, Feng Z and Xiao Y: miR-138 protects cardiomyocytes from hypoxia-induced apoptosis via MLK3/JNK/c-jun pathway. Biochem Biophys Res Commun 441: 763-769, 2013.
10. Lim JH, Lee YM, Chun YS, Chen J, Kim JE and Park JW: Sirtuin 1 modulates cellular responses to hypoxia by deacetylating hypoxia-inducible factor 1alpha. Mol Cell 38: 864-878, 2010.
11. Dioum EM, Chen R, Alexander MS, Zhang Q, Hogg RT, Gerard RD and Garcia JA: Regulation of hypoxia-inducible factor 2alpha signaling by the stress-responsive deacetylase sirtuin 1. Science 324: 1289-1293, 2009.
12. Rabinowitz JD and White E: Autophagy and metabolism. Science 330: 1344-1348, 2010.
13. Nakai A, Yamaguchi O, Takeda T, Higuchi Y, Hikoso S, Taniike M, Omiya S, Mizote I, Matsumura Y, Asahi M, *et al*: The role of autophagy in cardiomyocytes in the basal state and in response to hemodynamic stress. Nat Med 13: 619-624, 2007.
14. Liu L, Jin X, Hu CF, Li R, Zhou Z and Shen CX: Exosomes derived from mesenchymal stem cells rescue myocardial ischaemia/reperfusion injury by inducing cardiomyocyte autophagy Via AMPK and Akt pathways. Cell Physiol Biochem 43: 52-68, 2017.
15. Zhang H, Liu B, Li T, Zhu Y, Luo G, Jiang Y, Tang F, Jian Z and Xiao Y: AMPK activation serves a critical role in mitochondria quality control via modulating mitophagy in the heart under chronic hypoxia. Int J Mol Med 41: 69-76, 2018.
16. Kim J, Kundu M, Viollet B and Guan KL: AMPK and mTOR regulate autophagy through direct phosphorylation of Ulk1. Nat Cell Biol 13: 132-141, 2011.
17. Shore GC, Papa FR and Oakes SA: Signaling cell death from the endoplasmic reticulum stress response. Curr Opin Cell Biol 23: 143-149, 2011.
18. Zhao W, Han F and Shi Y: IRE1alpha pathway of endoplasmic reticulum stress induces neuronal apoptosis in the locus coeruleus of rats under single prolonged stress. Prog Neuropsychopharmacol Biol Psychiatry 69: 11-18, 2016.
19. Brozzi F, Nardelli TR, Lopes M, Millard I, Barthson J, Igoillo-Esteve M, Grieco FA, Villate O, Oliveira JM, Casimir M, *et al*: Cytokines induce endoplasmic reticulum stress in human, rat and mouse beta cells via different mechanisms. Diabetologia 58: 2307-2316, 2015.
20. Brozzi F, Gerlo S, Grieco FA, Juusola M, Balhuizen A, Lievens S, Gysemans C, Bugliani M, Mathieu C, Marchetti P, *et al*: Ubiquitin D regulates IRE1α/c-Jun N-terminal Kinase (JNK) protein-dependent apoptosis in pancreatic beta cells. J Biol Chem 291: 12040-12056, 2016.
21. Jain K, Suryakumar G, Ganju L and Singh SB: Amelioration of ER stress by 4-phenylbutyric acid reduces chronic hypoxia induced cardiac damage and improves hypoxic tolerance through upregulation of HIF-1α. Vascul Pharmacol 83: 36-46, 2016.
22. Liu B, Zhang HG, Zhu Y, Jiang YH, Luo GP, Tang FQ, Jian Z and Xiao YB: Cardiac resident macrophages are involved in hypoxiainduced postnatal cardiomyocyte proliferation. Mol Med Rep 15: 3541-3548, 2017.
23. Zheng W, Lu YB, Liang ST, Zhang QJ, Xu J, She ZG, Zhang ZQ, Yang RF, Mao BB, Xu Z, *et al*: SIRT1 mediates the protective function of Nkx2.5 during stress in cardiomyocytes. Basic Res Cardiol 108: 364, 2013.
24. Sommer RJ, Hijazi ZM and Rhodes JF: Pathophysiology of congenital heart disease in the adult: Part III: Complex congenital heart disease. Circulation 117: 1340-1350, 2008.
25. Zhu L, Wang Q, Zhang L, Fang Z, Zhao F, Lv Z, Gu Z, Zhang J, Wang J, Zen K, *et al*: Hypoxia induces PGC-1alpha expression and mitochondrial biogenesis in the myocardium of TOF patients. Cell Res 20: 676-687, 2010.
26. Zhu Y, Feng Z, Jian Z and Xiao Y: Long noncoding RNA TUG1 promotes cardiac fibroblast transformation to myofibroblasts via miR29c in chronic hypoxia. Mol Med Rep 18: 3451-3460, 2018.
27. Yan J, Duan J, Wu X, Guo C, Yin Y, Zhu Y, Hu T, Wei G, Wen A and Xi M: Total saponins from Aralia taibaiensis protect against myocardial ischemia/reperfusion injury through AMPK pathway. Int J Mol Med 36: 1538-1546, 2015.
28. Gu Y, Gao L, Chen Y, Xu Z, Yu K, Zhang D, Zhang G and Zhang X: Sanggenon C protects against cardiomyocyte hypoxia injury by increasing autophagy. Mol Med Rep 16: 8130-8136, 2017.
29. Liu MH, Lin XL, Guo DM, Zhang Y, Yuan C, Tan TP, Chen YD, Wu SJ, Ye ZF and He J: Resveratrol protects cardiomyocytes from doxorubicin-induced apoptosis through the AMPK/P53 pathway. Mol Med Rep 13: 1281-1286, 2016.
30. Hamid T, Gu Y, Ortines RV, Bhattacharya C, Wang G, Xuan YT and Prabhu SD: Divergent tumor necrosis factor receptor-related remodeling responses in heart failure: Role of nuclear factor-kappaB and inflammatory activation. Circulation 119: 1386-1397, 2009.
31. Milne JC, Lambert PD, Schenk S, Carney DP, Smith JJ, Gagne DJ, Jin L, Boss O, Perni RB, Vu CB, *et al*: Small molecule activators of SIRT1 as therapeutics for the treatment of type 2 diabetes. Nature 450: 712-716, 2007.
32. Vachharajani VT, Liu T, Brown CM, Wang X, Buechler NL, Wells JD, Yoza BK and McCall CE: SIRT1 inhibition during the hypoinflammatory phenotype of sepsis enhances immunity and improves outcome. J Leukoc Biol 96: 785-796, 2014.
33. Song S, Tan J, Miao Y, Li M and Zhang Q: Crosstalk of autophagy and apoptosis: Involvement of the dual role of autophagy under ER stress. J Cell Physiol 232: 2977-2984, 2017.
34. Thorburn A: Apoptosis and autophagy: Regulatory connections between two supposedly different processes. Apoptosis 13: 1-9, 2008.